



Quarkonium production in p–Pb collisions with ALICE

Igor Lakomov (for the ALICE collaboration)

CERN, CH-1211 Geneva 23, Switzerland

Abstract

The production of quarkonia, bound states of quark and anti-quark pairs, is intensively studied both experimentally and theoretically. They are ideal probes of the Quark-Gluon Plasma (QGP) formed in heavy-ion collisions. At the beginning of 2013, data from p–Pb collisions at $\sqrt{s_{NN}} = 5.02$ TeV have been collected by ALICE, which can be exploited to measure cold nuclear matter (CNM) effects on quarkonium production. These measurements are important in order to disentangle, in Pb–Pb collisions, hot and CNM effects. In this paper final ALICE results on the charmonium and bottomonium production in p–Pb collisions from Run I of the LHC are presented. ALICE measurements are compared to various models of CNM effects and to PHENIX measurements.

Keywords: ALICE, quarkonia, J/ψ , $\Psi(2S)$, $\Upsilon(1S)$, p–Pb, CNM effects, centrality, R_{pPb} , Q_{pPb} , p_T -broadening

1. Introduction

The suppression of quarkonia is considered as an ideal probe of the Quark-Gluon Plasma (QGP) formed in heavy-ion collisions. It was predicted that at sufficiently high energy densities the color screening of the heavy-quarks potential in deconfined QCD matter will lead to a sequential suppression of the production of different quarkonium states [1]. ALICE [2] is an LHC experiment dedicated to the study of QGP properties in heavy-ion collisions. ALICE has measured a suppression of J/ψ and $\Upsilon(1S)$ production in Pb–Pb collisions with respect to the expectations from pp collisions [3, 4, 5]. At the beginning of 2013, ALICE has collected the data from p–Pb collisions at $\sqrt{s_{NN}} = 5.02$ TeV. These data are important to measure cold nuclear matter (CNM) effects on quarkonium production. The evaluation of these effects allows, in Pb–Pb collisions, hot and CNM effects to be disentangled. CNM effects can be classified into initial (e.g. shadowing, saturation) and final (e.g. nuclear absorption, comover interaction) state effects. Some effects cannot be considered as purely initial or purely final state (e.g. coherent parton energy loss). Nuclear absorption is expected to be small at LHC energies due to the very short cross-

ing time of the heavy-quark pair. Final ALICE results on the charmonium and bottomonium production in p–Pb collisions from Run I are presented and compared to various models of CNM effects and to PHENIX results.

2. Analysis

Quarkonium production in ALICE is measured down to zero transverse momentum (p_T) in the e^+e^- channel (using central barrel detectors with pseudorapidity range $|\eta| < 0.9$) and in the $\mu^+\mu^-$ channel (employing the ALICE muon forward spectrometer with $-4 < \eta < -2.5$). At mid rapidity, the ALICE tracking system consists of the Inner Tracking System (ITS), including six layers of silicon detectors surrounding the beam pipe, and the Time Projection Chamber (TPC), a large cylindrical drift gas detector. The muon spectrometer consists of a front absorber, five tracking stations, a large 3 T m dipole magnet and two trigger chambers shielded by a muon filter wall. Minimum bias (MB) events were triggered by simultaneous signals in the two scintillator hodoscopes (V0) located at both sides of the interaction point (IP): $2.8 < \eta < 5.1$ and $-3.7 < \eta < -1.7$. Dimuon

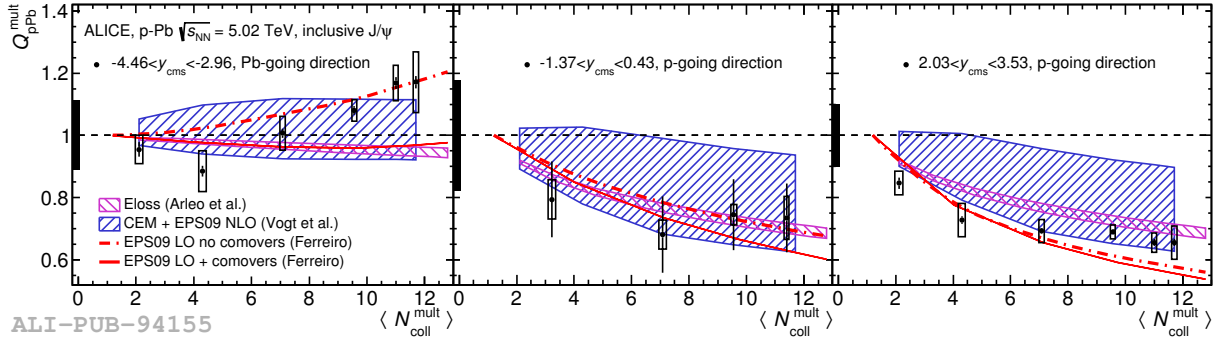


Figure 1: (Color online) Nuclear modification factor of J/ψ as a function of centrality in three rapidity ranges: backward (left), mid- (center) and forward (right) y intervals. The error bars show the statistical uncertainties and the boxes the uncertainties not fully correlated over $\langle N_{\text{coll}}^{\text{mult}} \rangle$. The black boxes at unity represent the uncertainties fully correlated over $\langle N_{\text{coll}}^{\text{mult}} \rangle$. Lines and bands are theoretical calculations from [6, 7, 8, 9].

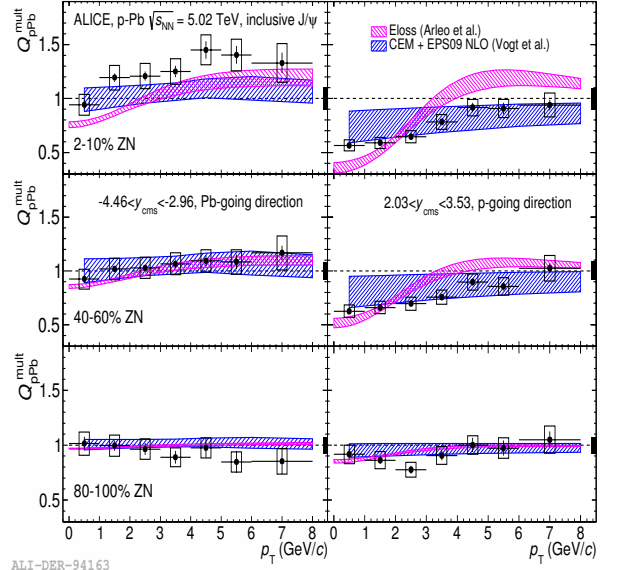
triggered events required, in addition to the MB condition, two opposite-sign muon tracks in the muon trigger chambers. Due to the beam-energy asymmetry during the p–Pb data-taking period, the nucleon-nucleon center-of-mass (cms) system is shifted in rapidity with respect to the laboratory frame by $\Delta y = 0.465$ towards the proton beam direction. The data have been taken with two beam configurations, obtained by inverting the directions of the p and Pb beams. This results in the following two y ranges measured with the muon spectrometer: backward ($-4.46 < y_{\text{cms}} < -2.96$) and forward ($2.03 < y_{\text{cms}} < 3.53$). Moreover, the mid- y range studied with central barrel detectors is not centered around zero: $-1.37 < y_{\text{cms}} < 0.43$. The used data samples correspond to integrated luminosities of 5 nb^{-1} , 5.8 nb^{-1} and $52 \mu\text{b}^{-1}$ for forward, backward and mid- y intervals. Finally, the event centrality is determined using the Zero Degree Calorimeters (ZDC) installed along the beam pipe at 112.5 m from the IP on both sides. Large fluctuations in a much lower particle multiplicity, together with the smaller range of participants in p–Pb collisions compared to Pb–Pb collisions, generate a dynamical bias on the centrality determination based on particle multiplicity usually used for this in Pb–Pb collisions [10]. Instead, the ZDC neutron energy distributions were used for the centrality determination in p–Pb collisions since these were found to be less sensitive to this dynamical bias. An additional assumption on the scaling of the mid- y charged hadron multiplicity $dN_{\text{ch}}/d\eta$ with N_{part} (number of participating nucleons) allowed the number of binary nucleon-nucleon collisions $N_{\text{coll}}^{\text{mult}}$ and the nuclear thickness function $T_{\text{pPb}}^{\text{mult}}$ in each centrality class to be determined. One of the main observables in quarkonium production analyses is the nuclear modification factor (R_{pPb}), the ratio of the quarkonium production

yield in p–Pb collisions to that in pp collisions scaled with N_{coll} . In the absence of nuclear effects this ratio is equal to 1. For the centrality-dependent studies in p–Pb collisions in ALICE it is referred to as $Q_{\text{pPb}}^{\text{mult}}$ due to the possible bias in the determination of $N_{\text{coll}}^{\text{mult}}$ (or $T_{\text{pPb}}^{\text{mult}}$). The centrality class 0–2% is excluded since this interval is contaminated by pile-up events (events with two or more inelastic p–Pb collisions superimposed). In the other centrality intervals the level of the pile-up does not exceed 3.5% decreasing towards peripheral collisions.

3. Results

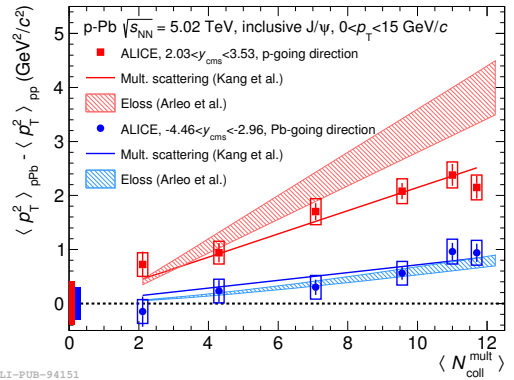
Results presented in these proceedings include those published by the ALICE Collaboration in [11, 12, 13, 14] and also the more recent ALICE results from [15]. First measurements of quarkonium production performed by ALICE in p–Pb collisions were discussed in [11] where a strong J/ψ suppression was found at forward y while at backward y the J/ψ production in p–Pb was consistent with that in pp collisions. Later, it was shown that the J/ψ suppression in p–Pb depends strongly on p_{T} at forward y while at backward and mid- y intervals no strong dependence was found [12]. Fig. 1 shows the $Q_{\text{pPb}}^{\text{mult}}$ of J/ψ as a function of centrality, integrated over p_{T} , measured in three rapidity intervals and compared to theoretical calculations for a pure shadowing model [6, 7], a shadowing model with comover contribution [8] and a coherent parton energy loss model [9]. Data indicate strong nuclear matter effects at backward and forward rapidities: $Q_{\text{pPb}}^{\text{mult}}$ increases with centrality at backward y but decreases at forward y . At mid- y the J/ψ suppression is similar to that at forward y however no strong conclusion can be done due to large experimental uncertainties. At back-

ward y , $Q_{\text{pPb}}^{\text{mult}}$ is consistent with 1 for the most peripheral and semi-peripheral events while at mid- and forward- y intervals a significant suppression of the J/ψ production in the full centrality range is seen. The models fairly agree with the data. Large theoretical uncertainties of shadowing models are dominated by the EPS09 shadowing parameterization. The shadowing model including a contribution from comover effect is presented without this uncertainty. It is shown as two lines including or not the comover effect. Inclusion of this effect into the shadowing calculations reduce $Q_{\text{pPb}}^{\text{mult}}$, especially in the most central collisions and at backward y . The shadowing model agrees better with the data if the comover effect is not included. The parton energy loss model has a smaller uncertainty band related to the variation of the gluon transport coefficient and to the parametrization of the production cross section. It also fairly agrees with the data except for the highest centrality region at backward y where it underestimates the measured $Q_{\text{pPb}}^{\text{mult}}$. It should be noted that ALICE measures the inclusive J/ψ production while theoretical calculations are given for the prompt J/ψ production. The fraction of J/ψ from B decays in the inclusive sample in p–Pb is similar to that in pp collisions ($\sim 10\%$) [16]. This effect is below the quoted experimental uncertainties [17]. Double-differential J/ψ production in p–Pb is shown in Fig. 2 as a function of p_T in different centrality intervals for backward- and forward- y ranges. A strong p_T dependence is found for the most central collisions, especially at forward y . For peripheral collisions $Q_{\text{pPb}}^{\text{mult}}$ is consistent with unity over the full p_T range in both backward and forward y regions. Theoretical models again show a fair agreement with the data. The parton energy loss model shows for the most central collisions at backward y slightly lower values of $Q_{\text{pPb}}^{\text{mult}}$ than seen in the data. At forward y for the most central collisions this model gives a stronger p_T dependence than seen in the data. ALICE also measured the centrality dependence of the p_T -broadening defined as $\Delta\langle p_T^2 \rangle = \langle p_T^2 \rangle_{\text{pPb}} - \langle p_T^2 \rangle_{\text{pp}}$ which is presented in Fig. 3. An important p_T -broadening is seen at backward and forward rapidities. While at backward y it has a similar magnitude as seen by PHENIX (not shown) in d–Au collisions at $\sqrt{s_{\text{NN}}} = 200$ GeV for all rapidities [20], at forward y , $\Delta\langle p_T^2 \rangle$ is higher by 1 – 1.5 $(\text{GeV}/c)^2$ in the full centrality range. The model based on multiple scattering [18, 19] shows almost perfect agreement with the data for both y intervals. The parton energy loss model shows a good agreement at backward y while at forward y it overestimates $\Delta\langle p_T^2 \rangle$ for the most central collisions. Another interesting measurement performed by ALICE is the $\psi(2S)$ R_{pPb} , integrated over



ALI-DER-94163

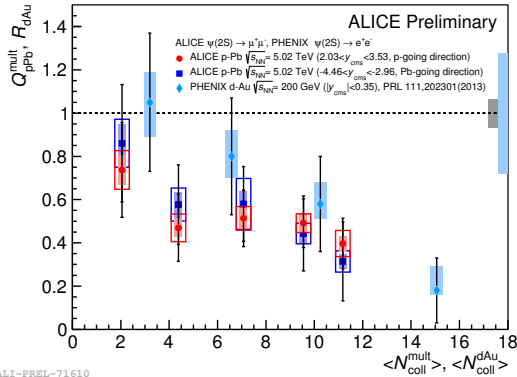
Figure 2: (Color online) Nuclear modification factor of J/ψ as a function of p_T at backward (left) and forward (right) y intervals, in three centrality ranges: 2-10% (top), 40-60% (center) and 80-100% (bottom). The error bars show the statistical uncertainties and the boxes the uncertainties not fully correlated over p_T . The black boxes at unity represent the systematic uncertainties fully correlated over p_T . Bands are theoretical calculations from [6, 7, 9].



ALI-PUB-94151

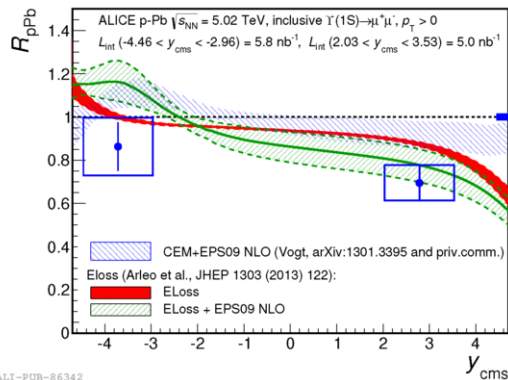
Figure 3: (Color online) Centrality dependence of $\Delta\langle p_T^2 \rangle$ of J/ψ for backward (blue circles) and forward (red squares) y . The error bars are the statistical uncertainties and the boxes the systematic uncertainties not fully correlated over centrality. Boxes at 1 represent uncertainties of the $\langle p_T^2 \rangle_{\text{pp}}$ interpolated to $\sqrt{s} = 5.02$ TeV and are fully correlated over centrality. The theoretical calculations are from [9, 18, 19].

p_T and centrality, which is found to be smaller than the J/ψ R_{pPb} , with a stronger difference at backward y . Comparison of the $Q_{\text{pPb}}^{\text{mult}}$ of $\psi(2S)$ measured by ALICE at $\sqrt{s_{\text{NN}}} = 5.02$ TeV with R_{dAu} measured by PHENIX at $\sqrt{s_{\text{NN}}} = 200$ GeV [22] as a function of $N_{\text{coll}}^{\text{mult}}$ and $N_{\text{dAu}}^{\text{dAu}}$, respectively, is presented in Fig. 4. Both mea-



ALI-PREL-71610

Figure 4: (Color online) Nuclear modification factor of $\psi(2S)$ as a function of N_{coll}^{mult} (N_{coll}^{dAu}) measured by ALICE (PHENIX) at backward (dark blue circles), forward (red squares) and mid- y (light blue diamonds). The error bars show the statistical uncertainties, open boxes the uncorrelated systematic uncertainties and the shaded boxes the partially correlated systematic uncertainties. Boxes at unity are correlated uncertainties for ALICE (grey) and PHENIX (light blue).



ALI-PUB-86342

Figure 5: (Color online) Nuclear modification factor of $\Upsilon(1S)$ as a function of y . The error bars represent the statistical uncertainties and the boxes the uncorrelated systematic uncertainties. Box at unity represents the correlated systematic uncertainty. The theoretical calculations are from [7, 21].

measurements show a similar increase of the $\psi(2S)$ suppression with centrality despite the different energies and y intervals. The coherent parton energy loss model [9] and the pure shadowing model [6, 7] cannot explain this effect since within these models the suppression of the $\psi(2S)$ and J/ψ will be similar. Final state effects are needed to be invoked to explain the different suppression. A model including suppression by comover interactions [8] is able to explain this difference for both ALICE and PHENIX. ALICE results on the $\Upsilon(1S)$ production in p–Pb collisions as a function of y [14] are presented in Fig. 5. At backward y , the $\Upsilon(1S)$ R_{pPb} is consistent with unity indicating no CNM effects. At for-

ward y a strong suppression of the $\Upsilon(1S)$ production in p–Pb collisions compared to that in pp is seen in the data. The shadowing [7] and the parton energy loss [21] models tend to overestimate the data and cannot simultaneously describe forward and backward y results.

4. Conclusions

Quarkonium production is measured in p–Pb collisions at $\sqrt{s_{NN}} = 5.02$ TeV by ALICE as a function of p_T , y and centrality for different quarkonium states. Strong p_T and centrality dependence of the J/ψ production is seen in the data which is fairly described by CNM models. Suppression of $\psi(2S)$ -to- J/ψ production is found in p–Pb compared to pp collisions which is consistent with the corresponding PHENIX d–Au results. Suppression of $\Upsilon(1S)$ production is found in p–Pb compared to pp collisions at forward y , while at backward y the data are consistent with no suppression.

References

- [1] T. Matsui, H. Satz, Phys.Lett. B178 (1986) 416.
- [2] B. B. Abelev, et al., Int.J.Mod.Phys. A29 (2014) 1430044. arXiv:1402.4476.
- [3] B. Abelev, et al., Phys. Rev. Lett. 109 (2012) 072301. arXiv:1202.1383.
- [4] B. B. Abelev, et al., Phys.Lett. B734 (2014) 314–327. arXiv:1311.0214.
- [5] B. B. Abelev, et al., Phys. Lett. B738 (2014) 361–372. arXiv:1405.4493.
- [6] R. Vogt, Phys.Rev. C81 (2010) 044903. arXiv:1003.3497.
- [7] J. Albacete, et al., Int.J.Mod.Phys. E22 (2013) 1330007. arXiv:1301.3395.
- [8] E. G. Ferreira, Phys. Lett. B749 (2015) 98–103. arXiv:1411.0549.
- [9] F. Arleo, et al., JHEP 1305 (2013) 155. arXiv:1304.0901.
- [10] J. Adam, et al., Phys. Rev. C91 (2015) 064905. arXiv:1412.6828.
- [11] B. B. Abelev, et al., JHEP 1402 (2014) 073. arXiv:1308.6726.
- [12] J. Adam, et al., JHEP 1506 (2015) 055. arXiv:1503.07179.
- [13] B. B. Abelev, et al., JHEP 1412 (2014) 073. arXiv:1405.3796.
- [14] B. B. Abelev, et al., Phys. Lett. B740 (2015) 105–117. arXiv:1410.2234.
- [15] J. Adam, et al. arXiv:1506.08808.
- [16] R. Aaij, et al., JHEP 1402 (2014) 072. arXiv:1308.6729.
- [17] B. B. Abelev, et al., JHEP 1402 (2014) 073. arXiv:1308.6726.
- [18] Z.-B. Kang, J.-W. Qiu, Phys.Lett. B721 (2013) 277–283. arXiv:1212.6541.
- [19] Z.-B. Kang, J.-W. Qiu, Phys.Rev. D77 (2008) 114027. arXiv:0802.2904.
- [20] A. Adare, et al., Phys.Rev. C87 (2013) 034904. arXiv:1204.0777.
- [21] F. Arleo, S. Peigné, JHEP 1303 (2013) 122. arXiv:1212.0434.
- [22] A. Adare, et al., Phys.Rev.Lett. 111 (2013) 202301. arXiv:1305.5516.